OPEN ACCESS

REGULAR ARTICLE

The Electronic Structure of the Cr:ZnS Crystal Modified by Mono- and Bi-Vacancy Defects

S.V. Syrotyuk^{1,*} , A.Y. Nakonechnyi¹, M.K. Hussain², Yu.V. Klysko¹, O.I. Shpak¹

Lviv Polytechnic National University, 79013 Lviv, Ukraine
Department of Electrical Power Techniques Engineering, AL-Hussain University College, 56001 Kerbala, Iraq

(Received 03 August 2025; revised manuscript received 15 October 2025; published online 30 October 2025)

The change in the electronic structure of a wide-gap semiconductor crystal ZnS with a Cr impurity replacing the zinc atom, i.e. Cr:ZnS, is considered. Two models of real crystals are built on the basis of this material. The first model contains a vacancy of a sulfur atom, i.e. V_S . The second model contains a bi-vacancy – of sulfur and zinc atoms, i.e. V_S , V_{Zn} . The study is devoted to establishing changes in the parameters of the electronic structure of the material caused by the influence of vacancies and bivacancies. The electronic structure of both materials was calculated within the frame-work of the full electron density functional (DFT) theory using the hybrid exchange-correlation functional PBE0. The use of the hybrid functional PBE0 is due to the presence of narrow energy bands with large values of the electron density of the 3d states on Cr atoms, for which the usual PBE-GGA functional is inapplicable. Significant differences in the parameters of the electronic energy structure were found for materials with sulfur atom vacancies VS and with bivacancies (VS, VZn). It was established that the material with a monovacancy is a semiconductor for both electron spin polarizations. It was found that the material with a bivacancy is a semimetal. The magnetic moments of both supercells are 4 μ_B .

Keywords: Cubic ZnS crystal, Cr impurity, Mono-vacancy, Bi-vacancy, Electronic structure, Magnetic moment.

DOI: 10.21272/jnep.17(5).05003 PACS numbers: 71.15.Mb, 71.20.Nr, 71.27. + a

1. INTRODUCTION

ZnTS materials, where T is a transition 3d element, are actively studied by theoretical and experimental methods [1].

The ZnS and Cu doped ZnS nanoparticles are synthesized by green hydrothermal method. Uniform, adherent and conducting thin films are obtained by simple spin coating. The X-ray diffraction studies show that the Cu ions are well dispersed into the ZnS lattice without changing the host crystal structure. It is observed that the transparency and conductivity change significantly with the Cu concentration in ZnS due to free carrier absorption and diffused crystallinity. The intrinsic ZnS thin film is found to be more transparent and conducting of the order of 10^{-4} mA and Cu doped ZnS films have lower band gap and conducting of the order of 10^{-11} mA. These have applications in high frequency UV light detectors, electroluminescent and optoelectronic devices [2].

Density-functional theory has been applied to investigate the electronic and magnetic properties of the pure and chromium-doped ZnS nanosheets via examining a number of important indicators including the electronic band structure and density of states. It is found that the pure nanosheet is a semiconductor with a band gap of about 2.525 eV. Moreover, the effect of doping the

chromium atom is manifested in the form of reduction in the value of the band gap to 1.85 eV, which results in half-metallic properties for the ZnS nanosheet. Most importantly, it is verified that the chromium-doped nanosheet has an intermediate band, which can be utilized in fabricating more advanced solar cells with a high rate of photon absorption and state-of-the-art lasers with a high quantum performance [3].

It was established that $Zn_{1-x}Fe_xS$ (x = 0, 0.1, 0.2) has two peaks, one in the violet region at 425 and the other in the blue region at 470 nm. The first emission is due to anion vacancy (Vs) which works as common electron trap under the conduction band edge and hole traps like cation vacancies (VZn), surface states (SS), which are in lower energy states, while the second emission is due to the transition from Vs to VZn. Furthermore, nano ZnS:Fe synthesized by a refluxing route showed a blue emission around 442 nm and its intensity dramatically also decreased as the amount of Fe doping increased, which is the general trend in II-VI compound semiconductors doping with Fe. Furthermore, Fe doping wurtzite ZnS nano particles exhibited blue and red emissions. A red shift of PL spectra is also reported with rising of Fe amount which implies that the increase in charge carrier leads to an enlargement of magnetic moment and as a result, the PL emission peak is red shifted. The

2077-6772/2025/17(5)05003(6)

05003-1

https://jnep.sumdu.edu.ua

^{*} Correspondence e-mail: stepan.v.syrotiuk@lpnu.ua

quenching of PL intensity in a doped sample with Fe is due acting of Fe ions as quenching centers of fluorescence; Fe works as an electron trapping center which out from nonradiative recombination. In the word, the photo-excited electrons prefer to translate to Fe metal ion causing traps centers as compare with the anion vacancy defect center. Kole et al doped ZnS with 1.1 at.% Mn and studied the influence of annealing on PL characterization. The prepared sample exhibited two emissions one in UV and one in orange regions, when the sample prepared at 400°C, the visible PL emission intensity decreased while the UV emission increased. Sakthivel et al prepared Zn_{0.98}Mn_{0.02}S by coprecipitation route and they found it emitted UV emission only. Hu et al studied the effect of different Mndoped concentration up to 0.9% on the PL emission of ZnS quantum doped prepared by the hydrothermal method.18 They found that the system emitted four peaks in blue and green regions located at 466, 495, 522, and 554 nm. Also, they examined the effect of annealing temperature on optical characteristics of ZnS: Mn (0.6 at.%) QDs; the PL of the annealed samples emitted four peaks emissions also in blue and green regions. The blue emissions are caused by the defect related emission of the ZnS host or transition from the conduction band to the zinc vacancies (VZn) level or sulfur dangling bonds at the interface of ZnS QDs or trap states emission of ZnS, related with native zinc vacancy (VZn). Previously, an intense peak at (352, 360, 365 nm) in violet region and 468 nm in blue region are observed in ZnS doped with Co due to the defect sites such as, sulfur vacancy and interstitial sulfur lattice defects. Also, the PL intensity is reduced with raising the cobalt amount [4].

With the rapid development of society, a series of energy crises and environmental pollution problems have arisen. Light is regarded as the ideal environmentally friendly reagent. Photocatalysis is an emerging green technology using sunlight, whichis considered to be one of the best solution store solve problems such as environmental pollution and energy depletion. However, many photocatalysts have low photocatalytic efficiency and serious photogenerated charge recombination, which hinders the overall efficiency and application scope of photocatalysis. In the past few decades, photocatalytic technology has been fully studied, but more exploration is needed to improve photocatalytic performance. After exploration and research, it has been found that vacancies have achieved remarkable achievements in the field of photocatalysis, and the important role of vacancies in improving photocatalytic performance has been confirmed. During the formation of vacancies, the adsorption and activation of reactants can be enhanced by inducing active sites, and the selectivity of surface reaction pathways and photocatalytic reactions can be regulated by the adsorption and dissociation of reaction intermediates on vacancies. Based on the above two points, vacancy engineering enhances photoreaction kinetics. The catalysts used in the photocatalytic reaction are generally mainly oxides and chalcogenides, so

sulfides are important parts of semiconductor catalytic materials. Metal sulfides are semiconductor compounds, and metal ions exist in various forms. Notably, metal sulfides have suitable electronic band gaps, small valence bands, exposed active sites, and exhibit strong quantum size effects. The physical, chemical, and optical properties of metal sulfide nanocrystals are easily tunable. However, the photocorrosion in the presence of metal sulfide limits its development. To prevent the photocorrosion of metal sulfide, researchers avoid the photocorrosion problem of metal sulfides themselves through strategies such as vacancy and doping. Therefore, metal sulfides have become the most popular class of photocatalysts for realizing visible light hydrogen evolution, degradation, and other applications. Vacancy engineering is a further effective strategy to tune interfacial interactions to promote the dynamic properties of charge carriers. In particular, sulfur vacancies, as a common vacancy, have been extensively studied. In recent years, the number of related papers on sulfur vacancy photocatalysts has also shown a clear upward trend. Researchers have studied the generation methods of sulfur vacancies and explored different synthetic routes, such as hydrothermal methods, in situ methods, solvothermal methods, etc. Researchers also investigated how sulfur vacancies are created during the material's synthesis. Not only that, researchers also investigated the different roles of sulfur vacancy engineering on enhancing photocatalytic performance; for example, expanding the light absorption range, promoting carrier separation, and improving surface reactions. The application of different metal sulfide photocatalysts, as well as the principle and advantages of sulfur vacancies in improving photocatalytic performance were also studied [5].

Customizing the chromatic discharge of nanomaterials is crucial for their use in light-emitting screens, field emitters, lasers, sensors, and optoelectronic devices. ZnS nanocrystals exhibit blue, green, and orange emissions. The luminescence characteristics of ZnS particles have been altered by doping with various transition elements and rare-earth metals. The optical characteristics are affected by defects, crystal structure, size, and shape. These studies show the ability to ad-just several emission characteristics from pure ZnS nanocrystals with various defect features [6].

ZnS doped with various elements are creating a new era for both academic research and industrial applications. So, the optical properties of modified ZnS thin film will help us to find a suitable doping element for convenient deposition which may enhance the conductance and transmitting properties of the film. For example, FE, FET, Catalytic, Solar cell, Electroluminescence, Fuel cell, different sensors (Chemical sensors, Biosensors, Humidity sensors, light sensors, UV light sensors) and nanogenerators use ZnS thin film [7].

Peculiarities of the impact of transition d elements on the electronic structure of wide-gap cubic crystals were

studied in theoretical works [8-10].

However, there are very few publications dedicated to the electronic structure of the materials ZnTS, containing the sulphur vacancies, VS. That is why the purpose of this study is to identify the changes in the electronic structure of wurtzite solid solutions T:ZnS caused by impurities of transition elements T. Only a few works have been published for these materials [11-12].

The problem of calculating the electronic structure of the wurtzite solid solution ZnS with an admixture of Cr and also with an S vacancy is relevant, and we proceed to its solution.

2. CALCULATION

The electronic structure of the supercell Zn₃₁Cr₁S₃₂ has been evaluated by means of the Abinit [13] code. Calculations of the electronic structure were performed here on the PAW (projector augmented waves) basis [14]. The PAW approach has common features with pseudopotential and full potential methods.

The calculation scheme in the PAW formalism is completed by obtaining an all-electronic wave function $|\psi_{\alpha k}\rangle$. The latter is derived from the smooth pseudo-wave function of the state $|\psi_{\alpha k}\rangle$. Here α is a band index, and \mathbf{k} is a vector from the first Brillouin zone. The true all-electronic wave function $|\psi_{\alpha k}\rangle$ is derived by acting of the operator τ on the smooth pseudo-wave function $|\psi_{\alpha k}\rangle$ [14],

$$|\psi_{\alpha \mathbf{k}}\rangle = \tau |\tilde{\psi}_{\alpha \mathbf{k}}\rangle$$
 (1)

The operator τ is buit on the free atom solutions. In particular, these functions are partial atomic waves ϕ , pseudowaves $\tilde{\phi}_i$ and projectors \tilde{p}_i . So, the operator τ is defined on these states and has the following form [14]:

$$\tau = 1 + \sum_{i} (\mid \varphi_{i} > - \mid \tilde{\varphi}_{i} >) < \tilde{p}_{i} \mid \tag{2}$$

The effective Hamiltonian H_{eff} is derived from the all electron Hamiltonian H by means the similarity transformation, based on a τ operator, namely

$$H_{eff} = \tau^{+} H \tau \tag{3}$$

The pseudowave function $|\psi_{\alpha k}\rangle$ is the eigenstate of the H_{eff} operator, namely:

$$H_{eff} \mid \tilde{\psi}_{\alpha \mathbf{k}} \rangle = \tau^{+} \tau \mid \tilde{\psi}_{\alpha \mathbf{k}} \rangle \varepsilon_{\alpha \mathbf{k}} \tag{4}$$

The energy eigenvalues ε_{ch} , derived from the system of linear equations (4), are identical to those evaluated from the all electron Hamiltonian H:

$$H \mid \psi_{\alpha \mathbf{k}} \rangle = \varepsilon_{\alpha \mathbf{k}} \mid \psi_{\alpha \mathbf{k}} \rangle \tag{5}$$

Having the all-electronic wave function $\psi_{\alpha {\bf k}}$, we can calculate the matrix elements of dipole transitions

$$\mathbf{d}_{fi} = \int \psi_f^* \sum_j e_j \mathbf{r}_j \psi_i d\tau$$
 necessary to evaluate the optical

properties of materials [15], the transport coefficients of semiconductors [16], as well as the splitting of the degenerate energy levels of an atom by an external electric field [17].

The 3d electrons of the Cr atom move in narrow energy bands and are characterized by large effective mass values. This means that the usual exchange-correlation functional PBE [18], which takes into account the gradient corrections of the electron density, is not suitable for an adequate description of 3d electrons. That is why we use the hybrid exchange-correlation functional PBE0 here. The latter is employed in the following form [19], namely

$$E_{xc}^{PBE0}[\rho] = E_{xc}^{PBE}[\rho] + \beta (E_x^{HF}[\Psi_{3d}] - E_x^{PBE}[\rho_{3d}]) \quad (6)$$

In this functional, the exchange-correlation energy of the 3d electrons of the Cr atom E_x^{PBE} , found in the GGA approximation, is partially removed, and the exchange energy of the same electrons, found in the Hartree-Fock theory E_x^{HF} , is substituted in its place.

Namely, the PBE0 functional is a mixture of two exchange-correlation functionals. The first of them is the usual GGA functional. It is suitable for smoothly varying electron densities in space. The second term in Eq. (5) contains the Hartree-Fock energy, in which there is no self-interaction error, which is very large for electrons that move in narrow energy bands, namely 3d electrons. The mixing factor β is recommended to be 0.25 [19].

3. RESULTS AND DISCUSSION

The calculated electronic properties of the Cr:ZnS solid solution in which the Cr atom replaces the Zn atom, are shown in Figs. 1–5.

Fig. 1 shows the majority-spin electronic energy bands, evaluated for supercells Zn31Cr1S32 with the S monovacancy (Vs) and with the bi-vacancy (Vs, Vzn) defects. For both these materials, for the majority spin, the fundamental gaps equal to 0.94 and 0.0 eV, respectively. And, for the minority spin the fundamental gaps equal to 1.19 and 0.43 eV, respectively. So, the material Cr:ZnS with the S mono vacancy defects, represented by a supercell Zn₃₁Cr₁S₃₂ reveals the semiconductor properties for the charge carriers with both spin orientations. The material Cr:ZnS with the bi-vacancy defects reveals the semiconductor properties for a minority spin and shows the metallic properties for a majority spin. As can be seen from Fig. 1 the Fermi level intersects the dispersion curves of charge carriers that move in very narrow energy bands. Both materials are the direct-gap semiconductors. Fig. 2 shows the minority-spin electronic energy bands. As can be seen from Fig. 2 the Fermi level is also situated within the forbidden band gap.

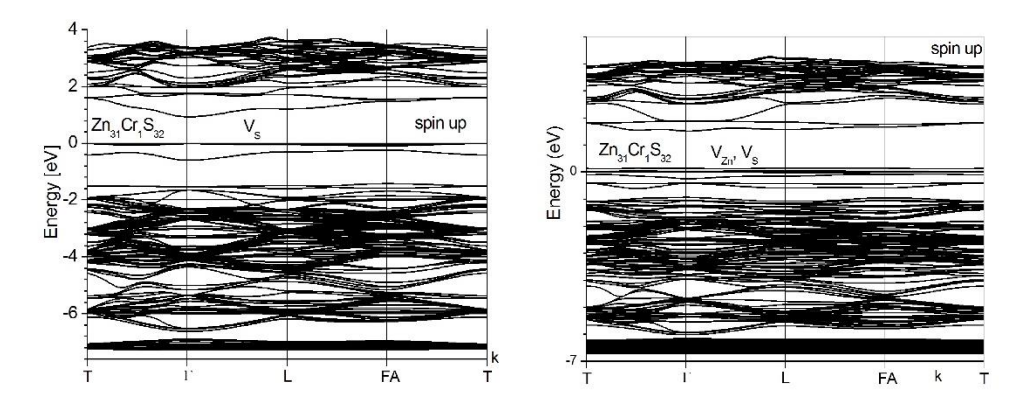


Fig. 1 – The majority-spin electronic energy bands, with the vacancies (Vs) and (Vzn, Vs), evaluated for supercell Zn₃₁Cr₁S₃₂

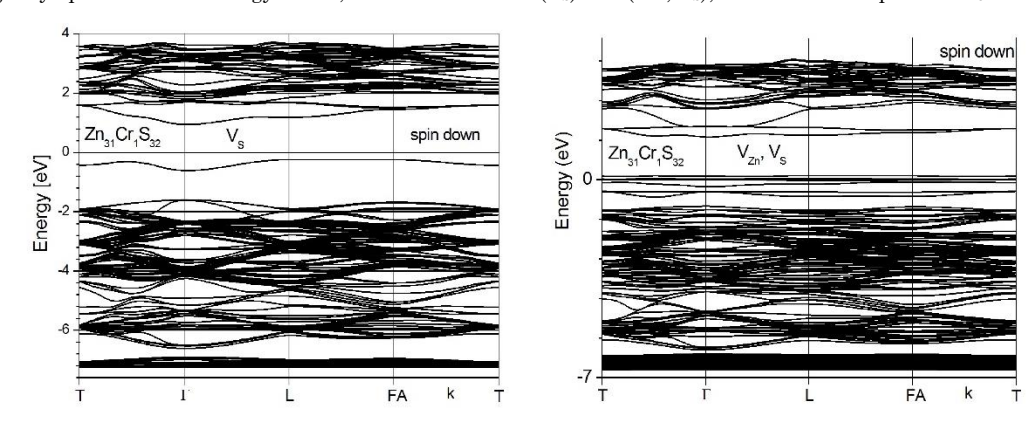


Fig. 2 – The minority-spin electronic energy bands, with the vacancies (Vs) and (Vzn, Vs), evaluated for supercell Zn₃₁Cr₁S₃₂

Curves in Fig. 3 reveal a significant asymmetry of the Cr d states, which indicates the presence of a non-zero magnetic moment of the supercell. For both supercells considered here, their total magnetic moments are 4.0 μ_B , and the contributions of Cr atoms are also approximately equal to 2.99 and 2.70 μ_B , for material mono- and bivacancy, respectively.

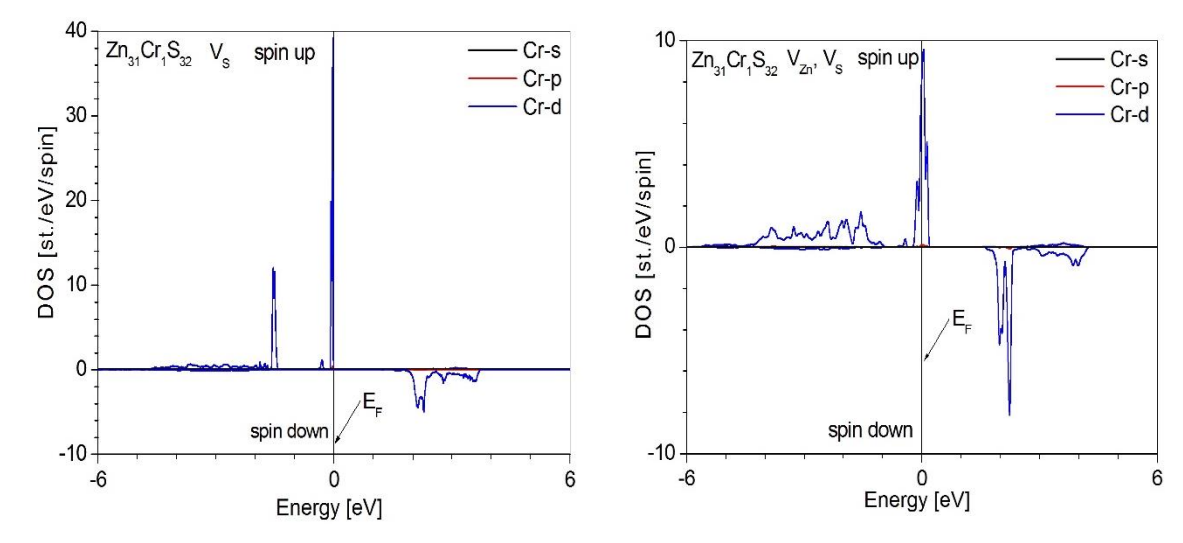
The partial densities of states on Zn and S atoms, presented in Fig. 4, show that the valence band is formed mainly by S p-states. However, Zn atoms mainly delegate s states to the conduction zone. We also note in Fig. 3 narrow energy bands of d symmetry in the valence band, which are characterized by large values of the density of electronic states. For an adequate description of such states, we employ the PBE0 hybrid exchange-correlation functional. The usual GGA functional is unsuitable for describing electrons moving in narrow energy bands of d symmetry. It is these charge carriers that are characterized by a large amount of self-interaction energy, partially excluded in the PBE0 functional. The asymmetry of the partial DOS curves, as well as the total density of electronic states (Fig. 5), is the result of the influence of the transition element Cr on the polarization of the electron density, even on such non-magnetic elements as Se and S.

4. CONCLUSION

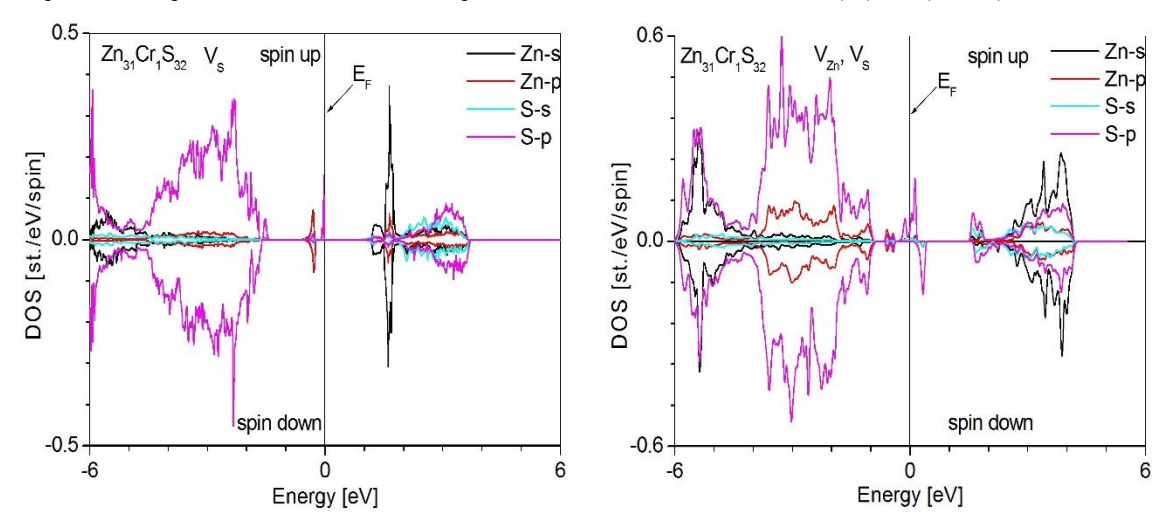
The spin-polarized electronic structure of the Cr:ZnS material, where the Zn is replaced by the Cr atom, is investigated. Electronic energy bands were evaluated for Zn₃₁Cr₁S₃₂ with the S monovacancy (V_S) and the Zn and S bivacancies (Vzn, Vs). The Cr impurity causes significant changes in the electronic structure of the ZnS crystal. However, the introduction of an additional point defect, namely a vacancy at the S atom site, leads to even greater changes in the electronic structure parameters. Thus, the fundamental band gap for the spin-up charge carrier equals to 0.94 eV, and for the spin-down states it is 1.19 eV. In a crystal with bivacancies, a radically different picture of the electronic energy structure is observed. In particular, for spin-up states, the material exhibits metallic properties. And for spin-down states, the material behaves like a semiconductor, with a fundamental gap value of 0.43 eV.

ACKNOWLEDGEMENTS

This contribution was created under the support of the High Performance Computing Laboratory at the Lviv Polytechnic National University.



 $\textbf{Fig. 3}-The\ spin-resolved\ partial\ DOS,\ evaluated\ for\ supercell\ Zn_{31}Cr_{1}S_{32},\ with\ the\ vacancies\ (V_S)\ and\ (V_{Zn},\ V_S)$



 $\textbf{Fig. 4}-The\ spin-resolved\ partial\ DOS,\ evaluated\ for\ supercell\ Zn_{31}Cr_1S_{32},\ with\ the\ vacancies\ (V_S)\ and\ (V_{Zn},\ V_S)$

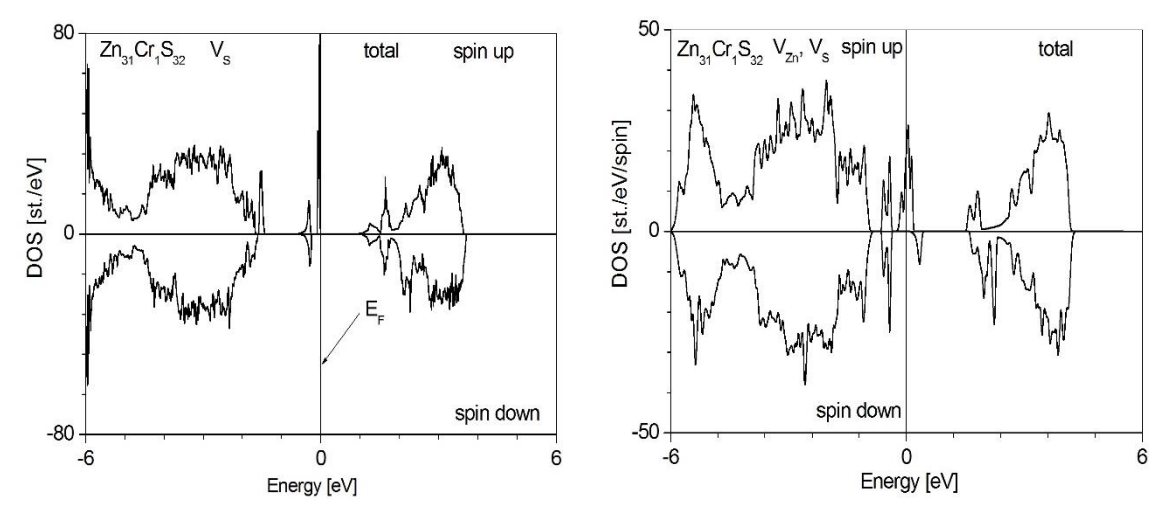


Fig. 5 – The spin-resolved total DOS, evaluated for supercell $Zn_{31}Cr_1S_{32}$, with the vacancies (V_S) and (V_{Zn}, V_S)

REFERENCES

- V.H. Choudapur, S.B. Kapatkar, A.B. Raju, J. Nano Electron. Phys. 11 No 5, 05017 (2019).
- 2. M. Jafari, Kh Alvani, *Mater. Res. Express* 6, 0850b5 (2019).
- 3. M.B. Mohamed, Int J Appl Ceram Technol., 00:1–9 (2019).
- Na Zhang, Z. Xing, Z. Li, W. Zhou, Chem. Catalysis 3, 100375 (2023).
- S.V. Syrotyuk, M.K. Hussain, *Physics and Chemistry of Solid State* 22, 529 (2021).
- S.V. Syrotyuk, O.P. Malyk, J. Nano Electron. Phys. 11 No 1, 01009 (2019).
- S.V. Syrotyuk, O.P. Malyk, J. Nano- and Electron. Phys., 11 No 6, 06018 (2019).
- S.V. Syrotyuk, I.V. Semkiv, H.A. Ilchuk, V.M. Shved, Condensed Matter Physics 19, 43703, 1 (2016).
- M. Labair, H. Rached, D. Rached, S. Benalia, B. Abidri, R. Khenata, R. Ahmed, S. Bin Omran, A. Bouhemadou, S.V. Syrotyuk, *Int. J. Mod. Phys. C*, 27, 1650107 (15) (2016).
- S.V. Syrotyuk, M.K. Hussain, J. Nano- and Electron. Phys. 15 No 5, 05002 (2023).
- S.V. Syrotyuk, A.Y. Nakonechnyi, Yu.V. Klysko, M.V. Stepanyak, V.M. Myshchyshyn, J. Nano- and Electron. Phys. 16 No 5, 05033 (2024).
- 12. S.V. Syrotyuk, A.Y. Nakonechnyi, Yu.V. Klysko, Z.E. Veres, I.I. Lahun, *J. Nano Electron. Phys.* 16 No 1, 01016 (2024).

- 13. X. Gonze, F. Jollet, F. Abreu Araujo, D. Adams, B. Amadon, T. Applencourt. C. Audouze, J.-M. Beuken. A. Bokhanchuk, E. Bousquet, F. Bruneval, D. Caliste, M. Cote, F. Dahm, F. Da Pieve, M. Delaveau, M. Di Gennaro, B. Dorado, C. Espejo, G. Geneste, L. Genovese, A. Gerossier, M. Giantomassi, Y. Gillet, D.R. Hamann, L. He, G. Jomard, J. Laflamme Janssen, S. Le Roux, A. Levitt, A. Lherbier, F. Liu, I. Lukacevic, A. Martin, C. Martins, M.J.T. Oliveira, S. Ponce, Y. Pouillon, T. Rangel, G.-M. Rignanese, A.H. Romero, B. Rousseau, O. Rubel, A.A. Shukri, M. Stankovski, M. Torrent, M.J. Van Setten, B. Van Troeye, M.J. Verstraete, D. Waroquier, J. Wiktor, B. Xu, A. Zhou, J.W. Zwanziger, Comput. Phys. Commun. 205, 106 (2016).
- 14. P.E. Blöchl, *Phys. Rev. B* **50**, 17953 (1994).
- S.V. Syrotyuk, Yu.V. Klysko, J. Nano Electron. Phys. 12 No 5, 05018 (2020).
- O.P. Malyk, S.V. Syrotyuk, J. Nano Electron. Phys. 14 No 1, 01014 (2022).
- I.O. Vakarchuk, Quantum Mechanics, Ivan Franko National University, Lviv, 2012, pp. 872.
- J.P. Perdew, K. Burke, M. Ernzerhof, *Phys. Rev. Lett.* 77, 3865 (1996).
- F. Tran, P. Blaha, K. Schwarz, P. Novák, *Phys. Rev. B* 74, 155108 (2006).

Електронна структура кристала Cr:ZnS, модифікована моно- та бівакансіями

С.В. Сиротюк¹, А.Й. Наконечний¹, М.К. Hussain², Ю.В. Клиско¹, О.І. Шпак¹

¹ Національний університет «Львівська політехніка», 79013 Львів, Україна ² Department of Electrical Power Techniques Engineering, AL-Hussain University College, 56001 Kerbala, Iraq

Розглядається зміна електронної структури широкозонного напівпровідникового кристала ZnS з домішкою Cr, яка заміщує атом цинку, тобто Cr:ZnS. На основі цього матеріалу побудовані дві моделі реальних кристалів. Перша модель містить вакансію атома сірки, тобто VS. Друга модель містить подвійну вакансію – атомів сірки та цинку, тобто VS, VZn. Дослідження присвячене встановленню змін параметрів електронної структури матеріалу, спричинених впливом вакансій та бівакансій. Електронна структура обидвох матеріалів обчислювалась в рамках теорії функціонала повної електронної густини (DFT) з використанням гібридного обмінно-кореляційного функціонала PBE0. Застосування гібридного функціонала PBE0 зумовлене наявністю вузьких енергетичних зон з великими значеннями густини електронів 3d симетрії атомів Cr, для яких звичайний функціонал PBE-GGA незастосовний. Виявлено суттеві відмінності параметів електронної енергетичної структури, знайдені для матеріалів з вакансіями атома сірки Vs та з бівакансіями (Vs, Vzn). Встановлено, що матеріал з моновакансією є напівпровідником для обидвох спінових поляризацій електронів. Виявлено, що матеріал з бівакансією є напівметалом. Магнітні моменти обидвох надкомірок складають 4 μ в.

Ключові слова: Кубічний кристал ZnS, Домішка Cr, Моновакансія, Бівакансія, Електронна структура, Магнітний момент.